In Vivo Proton MR Spectroscopy of Primary and Nodal Nasopharyngeal Carcinoma

Ann D. King, David K.W. Yeung, Anil T. Ahuja, S.F. Leung, Gary M.K. Tse and Andrew C. van Hasselt

AJNR Am J Neuroradiol 2004, 25 (3) 484-490
http://www.ajnr.org/content/25/3/484

AJNR Am J Neuroradiol 25:484–490, March 2004

In Vivo Proton MR Spectroscopy of Primary and Nodal Nasopharyngeal Carcinoma

Ann D. King, David K.W. Yeung, Anil T. Ahuja, S.F. Leung,
Gary M.K. Tse, and Andrew C. van Hasselt

BACKGROUD AND PURPOSE: **The aim of this study was to determine the feasibility of performing in vivo proton (^{1}H) MR spectroscopy of nasopharyngeal carcinoma (NPC) and to document the ^{1}H spectrum of this cancer.**

METHODS: **Twenty-seven patients with NPC lesions >1 cm^3 underwent localized ^{1}H MR spectroscopy performed at 1.5 T. Water-suppressed spectra from both primary tumors (nine cases) and metastatic nodes (18 cases) were obtained at TE 136 and 272. Spectra were analyzed in the time domain by using a nonlinear least squares fitting algorithm with incorporation of previous knowledge. Choline (Cho)/creatine (Cr) ratios for primary NPC and metastatic nodes were calculated and compared. Spectra from normal neck muscle of five volunteers were acquired as control data.**

RESULTS: **^{1}H MR spectroscopy was successfully obtained in seven (78%) of nine primary tumors and 16 (89%) of 18 metastatic nodes. Intense lipid signals in the range of 0.89 to 2.02 ppm were observed in 95% of spectra at TE 136 and 91% of spectra at TE 272. At TE 136, Cho/Cr for metastatic nodes (5.3 ± 1.6) was significantly higher than the ratio for primary (2.6 ± 0.5) NPC lesions (P = .02). Cho/Cr ratios for NPC lesions were higher than those for normal neck muscles, for which values ranged from 0 to 0.97 and 0 to 1.1 at TE 136 and 272, respectively.**

CONCLUSION: **^{1}H MR spectroscopy is a feasible technique for the evaluation of NPC tumors >1 cm^3. Cho/Cr ratios for the lesions were high compared with those for normal neck muscle.**

Proton (^{1}H) MR spectroscopy provides a noninvasive method for studying cellular metabolism. During the past few years, it has become an accepted tool for evaluating cancer. The results of ^{1}H MR spectroscopy have been reported most widely for brain tumors, but a large body of research is now accumulating for other cancers of the body, such as prostate, breast, ovary, cervix, and colon (1). However, because of the inherent problems in performing MR spectroscopy of the head and neck (shimming, strong lipid signal intensity, and low signal intensity-to-noise ratios), only a few in vivo cancer series have included ^{1}H MR spectroscopy in this region (2–5). To our knowledge, none have included ^{1}H MR spectroscopy for detection of nasopharyngeal carcinoma (NPC). ^{1}H MR spectroscopy has a large potential role in oncology, including detection of malignancy, grading tumor, predicting response to treatment, monitoring treatment response, and identifying persistent or recurrent disease. The first step in this process requires the identification of spectra associated with specific cancers.

With this study, we investigated the possibility of obtaining interpretable ^{1}H spectra in vivo from untreated patients with undifferentiated carcinoma of the nasopharynx by performing spectroscopy on either the primary or the metastatic cervical node. Attempts were made to obtain semi-quantitative measurement in terms of choline (Cho)/creatine (Cr) ratios with the use of a time domain spectral fitting technique that incorporates previous knowledge in the data analysis.

Methods

Patient Selection

Patients presenting with primary undifferentiated carcinoma of the nasopharynx, who had not received previous treatment, were recruited from one institution between November 2001 and February 2003 for this prospective study. Informed consent was obtained from all recruits. Those patients with primary

Received June 16, 2003; accepted after revision August 23.

From the Departments of Diagnostic Radiology & Organ Imaging (A.D.K., A.T.A.), Clinical Oncology (D.K.W.Y., S.F.L.), Anatomical and Cellular Pathology (G.M.K.T.), and Surgery Faculty of Medicine (A.C.v.H.), The Chinese University of Hong Kong, Prince of Wales Hospital, Shatin, New Territories, Hong Kong, Special Administrative Region, China.

Address reprint requests to A.D. King, Department of Diagnostic Radiology and Organ Imaging, Faculty of Medicine, The Chinese University of Hong Kong, Prince of Wales Hospital, Shatin, New Territories, Hong Kong, Special Administrative Region, China.

tumor or metastatic lymph node of >1 cm^3 were included in the study. Histologic diagnosis was made from biopsy of the primary nasopharyngeal tumor, and spectroscopic examination of primary tumors was performed at least 2 weeks after biopsy. Because normal nasopharyngeal tissues are too small to undergo spectroscopy, five normal volunteers were recruited to obtain control spectra from normal muscle in the neck. The local ethics committee granted ethical approval for the study.

MR Imaging Examination

The examinations were performed on a 1.5-T whole body MR imaging system. A standard volume head and neck coil was used for the imaging of the head and neck and for performing MR spectroscopy on the primary NPC. Additionally, a 20-cm-diameter circular receive-only surface coil placed over the neck was used to improve the signal intensity-to-noise ratio when performing MR spectroscopy of metastatic lymph nodes. The body coil was used to generate a homogeneous B_1 excitation field in all MR imaging examinations. MR imaging was performed in the transverse and coronal planes, and, with image guidance, the radiologist (A.D.K) positioned the volume of interest within each lesion, carefully excluding air and normal structures such as bone, muscle, and fat. If both the primary tumor and the node were of suitable size for spectroscopy, spectroscopy was performed preferentially on the primary tumor. When patients presented with bilateral or multiple lymph nodes, the largest node was selected for study.

Using the point-resolved spectroscopy sequence with either the head and neck coil or the circular surface coil selected as the signal intensity receiver, two water-suppressed spectra (2000/136 and 2000/272 [TR/TE]) were acquired for each volume of interest. The purposes of using two TE in this study were to verify whether lactate (Lac) (1.32 ppm) was present in NPC lesions, to examine the effect of longer TE on the visibility of metabolites of interests (Cho, 3.2 ppm; Cr, 3.03 ppm), and to learn whether lipid peaks (0.5 to 2.1 ppm), often present in the spectra of head and neck lesions, could be reduced by using longer TE. Pre-acquisition optimization procedures consisted of receiver gain and frequency adjustment, shimming, and gradient tuning. Water suppression was achieved by selective inversion recovery, starting the measurement at the zero crossing of the water signal intensity. Data were acquired at a spectral bandwidth of 1000 Hz, and 64 water-suppressed signals were acquired. The averaged signal intensity was exported and processed on an off-line computer.

Data Analysis

Spectra were visually assessed for the presence or absence of metabolites, including Cho, Cr, fatty acids (FA) (– CH_2 –) (2.02 ppm), FA (– CH_2 –) (1.30 ppm), FA (– CH_3) (0.89 ppm), and Lac (seen as an inverted doublet at TE 136 and back in phase at TE 272). A minimal signal intensity-to-noise ratio of 2:1 was required for a peak to be considered present in the spectrum. Spectral analysis was performed in the time domain by one physicist (D.K.W.Y.) with the use of a fitting routine known as the *advanced method for accurate, robust, and efficient spectral fitting*, or AMARES (6) implemented in the MRUI software package (available at www.mrui.uab.es/mrui/mruiHomePage.html). Both residual water (4.65 ppm) and the broad intense FA peaks in the chemical shift range of 0.89 to 2.02 ppm were first removed from the measured free induction decay by means of the time domain Hankel-Lanczos singular value decomposition filtering (7) to enable a more precise estimation of Cho and Cr peak areas.

As the starting values in the nonlinear least squares fitting algorithm, the manually selected resonance frequency and line width of Cho and Cr were used. Previous knowledge incorporated into the fitting procedure consisted of the following: line widths of Cr equal to those of Cho; resonance frequencies were constrained to lie in the range ±0.05 ppm of the peaks' known resonance frequencies; the zero and first-order phase correction estimated by AMARES were fixed to zero; and the resonances relative to the phase were also set to zero. The individual FA peaks were not quantified in this study because of lack of a satisfactory previous knowledge model to fit complex overlapping signals in the 0.89 to 2.02 ppm region that might also contain signal intensity contribution from other biochemicals. The calculated Cho and Cr peak areas were used to determine the Cho/Cr ratio for those lesions in which both the Cho and Cr peak could be determined by the fitting routine AMARES. The line widths of Cho as determined by the fitting algorithm and the estimated FA peak at 1.3 ppm were used to evaluate the quality of the spectra.

To test for differences in Cho/Cr values between primary NPC and metastatic nodes, in those lesions in which the Cho/Cr was measurable, we used the Mann-Whitney nonparametric test. The differences were considered significant when $P < .05$.

Results

Study Group

Twenty-seven patients (21 male and six female patients; age range, 38–65 years; mean age, 48 years) were recruited for the study. The histologic finding for all patients was NPC, World Health Organization type III, except for one type II lesion. For nine patients, ^{1}H MR spectroscopy was performed on the primary tumor by using voxel volumes of 2.4 to 9 cm^3 (mean, 4.8 cm^3), and for 18 patients, ^{1}H MR spectroscopy was performed on a metastatic node by using voxel volumes of 2 to 10.2 cm^3 (mean, 5.0 cm^3). Control spectra were obtained from the neck muscles of five volunteers (three male and two female volunteers; age range, 39–76 years; mean age, 55 years) by using voxel volumes of 4 to 10.8 cm^3 (mean, 6.9 cm^3).

^{1}H MR Spectroscopy

Table 1 summarizes the ^{1}H MR spectroscopy results for primary tumors and metastatic nodes acquired at TE 136 and 272. Both the primary tumor and the metastatic node spectra showed presence of broad and intense overlapping peaks derived from FA in the chemical shift range of 0.89 to 2.02 ppm, and those peaks were found to persist even at TE 272. No evidence of Lac was shown from the primary tumor and node spectra. Only five (22.7%) of the 22 successful spectra at TE 272 were found to contain Cr, whereas at TE 136, 13 (61.9%) of the 21 successful spectra were found to contain Cr. The number of non-interpretable spectra irrespective of TE was higher for primary tumors (27.8%) compared with metastatic nodes (16.7%).

Figure 1A shows the MR image of a patient with a primary NPC tumor; the corresponding ^{1}H spectrum shows presence of Cho and Cr peaks. Figure 2A shows the MR image of a patient with a metastatic node in which an intense Cho peak was detected but no Cr resonance was found. The mean Cho/Cr for all successfully evaluated NPC lesions (primary and node) was 4.5 ± 1.9 at TE 136 and 2.8 ± 0.8 at TE 272. At TE 136, Cho/Cr for nodes (5.3 ± 1.6) was

Results of in vivo proton MR spectroscopy of primary nasopharyngeal carcinoma and metastatic lymph nodes

					TE 136						TE 272					
Patient No.	Sex	Age (yr)	VOI (cm^3)	NPC Lesion	Cho/Cr	Cho 3.2	Cr 3.03	FA 2.02	FA 1.30	FA 0.89	Cho/Cr	Cho 3.2	Cr 3.03	FA 2.02	FA 1.30	FA 0.89
1	M	45	3.9	Primary	1.9	+	+	−	+	−	1.6	+	+	−	+	+
2	M	48	9	Primary		NI	NI	NI	NI	NI	ND	+	−	−	+	+
3	M	60	4.5	Primary	ND	−	−	−	+	+	ND	−	−	−	+	+
4	M	55	2.4	Primary	3.1	+	+	−	+	+	3.7	+	+	−	−	−
5	M	45	3	Primary		NI	NI	NI	NI	NI		NI	NI	NI	NI	NI
6	M	42	3.4	Primary	2.8	+	+	−	+	+	3.3	+	+	−	+	+
7	F	65	4.5	Primary		−	−	+	+	+		−	−	−	+	+
8	M	50	8.5	Primary	2.5	+	+	−	+	+	ND	+	−	−	+	+
9	M	45	3.6	Primary		NI	NI	NI	NI	NI		NI	NI	NI	NI	NI
10	M	48	5.4	Node		NI	NI	NI	NI	NI	ND	+	−	−	+	+
11	M	45	10.2	Node	6.9	+	+	−	+	+	ND	+	−	+	+	+
12	M	49	5.4	Node	4.2	+	+	−	+	+	ND	+	−	−	+	+
13	F	38	2.1	Node	6.3	+	+	−	+	+	ND	+	−	−	+	+
14	M	39	3.2	Node	7.5	+	+	−	+	+	ND	+	−	+	+	+
15	F	55	2.5	Node	ND	+	−	−	+	+	ND	+	−	−	+	+
16	M	46	5.1	Node	ND	+	−	−	+	+		NI	NI	NI	NI	NI
17	F	41	7.2	Node	5.8	+	+	−	+	+	ND	+	−	−	+	+
18	M	57	10.1	Node	5.1	+	+	−	+	+	ND	+	−	−	+	+
19	F	46	3.4	Node	5.4	+	+	−	+	+	ND	+	−	−	+	+
20	M	41	2	Node	ND	+	−	+	+	+	ND	+	−	+	+	+
21	M	51	5.4	Node	ND	+	−	−	+	+	ND	+	−	+	+	+
22	M	55	3.7	Node	ND	+	−	−	+	+	ND	−	−	−	+	+
23	M	42	6.5	Node	ND	+	−	−	−	−	3.1	+	+	−	−	−
24	F	48	3.2	Node	2	+	+	−	+	+	2.2	+	+	−	+	+
25	M	51	5.3	Node		NI	NI	NI	NI	NI		NI	NI	NI	NI	NI
26	M	51	5.2	Node	4.9	+	+	−	+	+	ND	+	−	−	+	+
27	M	45	3.3	Node		NI	NI	NI	NI	NI		NI	NI	NI	NI	NI

Note.—VOI indicates volume of interest; NPC, nasopharyngeal carcinoma; Cho, choline; Cr, creatine; FA, fatty acid; M, male; F, female; ND, not determined, mainly because creatine was not present or both choline and creatine were not detected in successfully obtained spectra; NI, not interpretable; +, metabolite present with a minimal signal-to-noise ratio of 2:1; −, metabolite absent. Numbers shown with the metabolites are chemical shift values in parts per million (ppm). All nasopharyngeal carcinoma lesions were of World Health Organization classification type III, except for the lesion in patient 26, which was type II.

significantly higher than the ratio for primary (2.6 ± 0.5) NPC lesions ($P = .02$).

The line width of the Cho peak seen in primary tumor spectra was 4.5 ± 0.4 Hz at TE 136 and 4.3 ± 0.8 Hz at TE 272. For nodes, the line width of Cho was 3.7 ± 0.6 Hz at TE 136 and 3.1 ± 0.8 Hz at TE 272. The lipid peak at 1.3 ppm was the most intense signal intensity of the three FA peaks detected in NPC and had a line width range of 5.8 to 13.5 Hz at TE 136 and 9.5 to 13.6 Hz at TE 272. No detectable Cho or Cr resonances were found in the neck muscle of two healthy volunteers, and the Cho/Cr ratios from the three remaining volunteers ranged from 0 to 0.97 at TE 136 and 0 to 1.1 at TE 272.

Discussion

NPC challenges many fields of medicine, from the molecular level of chromosome alterations, cancer-related genes, and the association with the Epstein–Barr virus to the difficulties of treating and managing cancer that involves vital structures at the skull base. ^{1}H MR spectroscopy has the potential to become another tool in expanding our understanding of this cancer, particularly for predicting the response to treatment and determining the nature of any residual mass that persists after radiation therapy. Our purposes were to examine whether ^{1}H MR spectroscopy of untreated NPC was feasible and to document the spectral characteristics of these lesions.

We found that ^{1}H MR spectroscopy of NPC was feasible considering that interpretable spectra were obtained from 67% of primary tumors and 83% of metastatic nodes at TE 136 in tumors >1 cm^3. From these spectra, Cho was the most commonly found metabolite, being present in four (67%) of six primary tumor spectra and in all (100%) metastatic node spectra. Cr was less frequently (60%) detected in node spectra compared with Cho, and at the longer TE, only 13% of the node spectra had detectable Cr (Fig 2B). The fall in the level of Cr below detectable levels at the longer TE (TE 272) was most likely caused by relaxation losses.

The use of previous knowledge in the spectral fitting procedure does improve the accuracy with which Cho and Cr peak areas are measured (Fig 1C). We obtained a Cho/Cr ratio for NPC (Cho/Cr ratio of 4.5 at TE 136) that was higher than the ratio obtained for normal muscle used as control in this study (Cho/Cr ratio of 0–1.1). Our results for the Cho/Cr ratio of

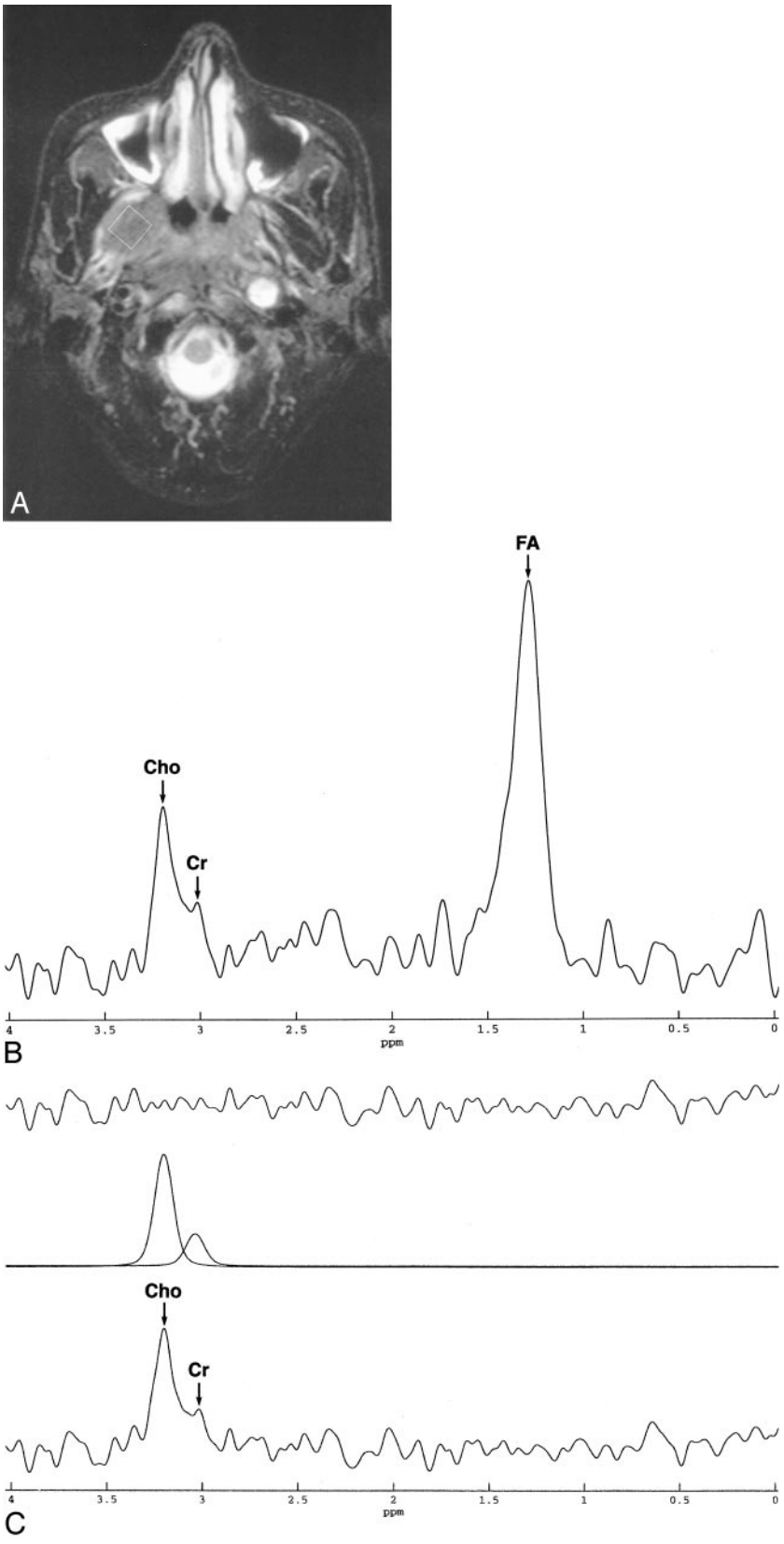

FIG 1. Images of patient 1.

A, Axial view fat-suppressed T2-weighted MR image shows the position of the volume of interest for spectroscopy represented by the *white square* placed within the primary NPC tumor.

B, Spectrum acquired at ^{1}H MR spectroscopy with TE 136 from the primary NPC tumor shown in *A*. The nominal voxel volume was 3.9 cm^3. Prominent peaks detected were Cho (3.2 ppm), Cr (3.03 ppm), and lipids (1.30 ppm).

C, Lipids were removed from the original spectrum shown in *B* with the use of Hankel-Lanczos singular value decomposition filtering before spectral fitting was performed (*bottom trace*). The fitted spectrum performed in the time domain is shown by the *middle trace*, and the *top trace* represents the residual signal intensity.

normal muscle acquired at a TE 136 were similar to the results obtained in other studies by Mukherji et al (3) (Cho/Cr ratio of 0–1.16 at TE 136) and Star-Lack et al (2) (Cho/Cr ratio of 0.55 ± 0.21 at TE 144). The high Cho/Cr ratio of cancer compared with that of normal muscle has also been observed in cases of squamous cell carcinoma of the extracranial head and neck (3, 8, 9), with a reported Cho/Cr range of 1.8 to

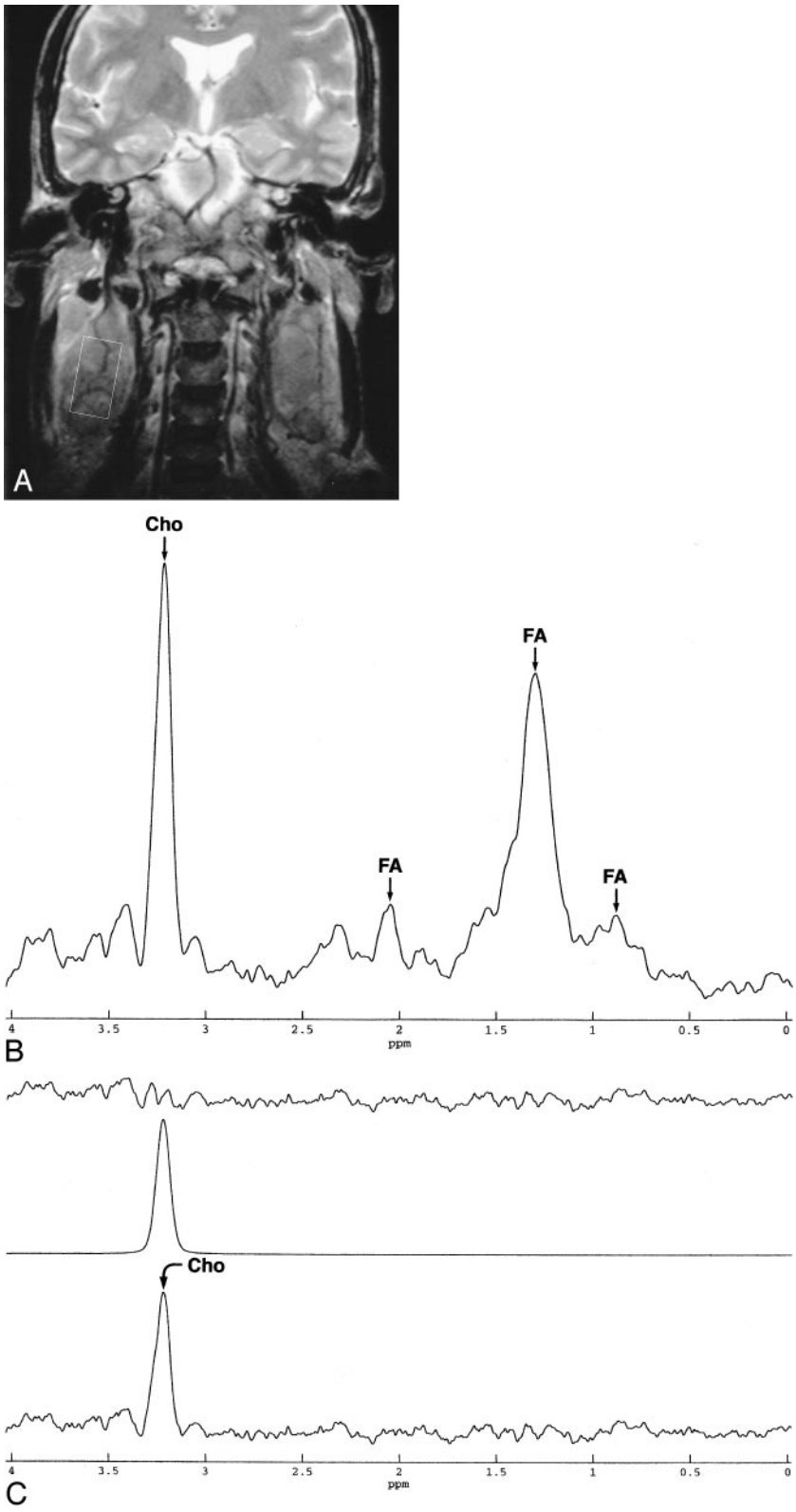

FIG 2. Images of patient 20 with NPC.

A, Coronal view T2-weighted MR image shows the position of the volume of interest for spectroscopy represented by the *white rectangle* placed within the metastatic lymph node.

B, Spectrum acquired at ^{1}H MR spectroscopy with TE 136 from the metastatic node. The nominal voxel volume was 2 cm^3. Both Cho (3.2 ppm) and methylene lipid (1.30 ppm) peaks were present, but Cr (3.02 ppm) was not clearly seen.

C, Lipids were removed from the original spectrum shown in *B* with the use of Hankel-Lanczos singular value decomposition filtering before spectral fitting was performed (*bottom trace*). The fitted spectrum performed in the time domain is shown by the *middle trace*. Only the intense Cho peak was successfully estimated, whereas the Cr peak was not found. The *top trace* represents the residual signal intensity.

7.2. The elevated Cho resonance at 3.2 ppm detected in vivo in NPC lesions is actually a composite peak and is thought to contain Cho, phosphocholine, phosphatidylcholine, and glycerophosphocholine (10). Cho and its derivatives are thought to originate from phospholipid metabolism of cell membranes. Elevation of this composite Cho peak has been found in several cancers (11, 12) and it is possible that it can be used as a marker for active cellular proliferation.

Although we were able to show that Cho/Cr ratios were higher in NPC lesions than in normal muscle tissue and that this ratio was significantly higher for

nodes compared with primary lesions, one limitation needs to be addressed. Because we used metabolite ratios in this study, we could not verify whether the observed Cho/Cr differences were due to changes to either one or both metabolites. To address this issue, absolute concentration measurements would have been necessary and would have required an additional signal intensity acquisition from a phantom containing a reference solution of known concentration. However, our results also showed that Cr was less commonly detected in metastatic nodes compared with primary tumor on spectra acquired with the same TE. The undetectable Cr may reflect a failure of the technique to obtain adequately resolved spectra, but this would not explain why Cr was found more frequently in the primary tumor, the region in which it was technically more difficult to perform MR spectroscopy. An alternate explanation may be that low or undetectable Cr reflects increased rate of metabolism associated with more aggressive tumor (13). It could be postulated that the carcinomas that have already spread to the nodes are the more aggressive ones and that, hence, this is why nodal metastases have less detectable Cr. This is only a hypothesis based on a small number of patients; further research would require direct comparison of the spectra of metastatic nodes and primary tumor from the same patient, together with correlation of ^{1}H MR spectroscopy with parameters such as grade of tumor and patient outcome.

In addition to Cho and Cr peaks, broad lipid signals were also detected in most primary tumor and node spectra. The significance of these lipid peaks is uncertain because they are associated not only with malignancy but also with necrosis, inflammation, and benign cellular processes (1). It is unclear whether the bulk of these detected lipids originated from within the cancer or was caused by signal intensity contamination from adjacent fatty tissues. In all cases, great care was taken to include only tumor in the voxel, but both the primary nasopharyngeal tumor lying adjacent to the parapharyngeal fat spaces and the metastatic nodes surrounded by fatty tissues are challenging areas for in vivo spectroscopy. However, because intense lipid signals have also been documented in ^{1}H spectra of the head and neck lesions acquired in vitro (14, 15), we postulate that the FA signals observed in our spectra originated from the lesions themselves. Nevertheless, further studies are needed to confirm their origin and to develop accurate models of previous knowledge to aid in the quantification of these peaks in vivo.

One of the reasons for using two TE in this study was to verify whether Lac could be found in NPC lesions. None of the spectra acquired in this study showed evidence of Lac, but we cannot rule out the presence of this metabolite from NPC lesions for two reasons. First, Lac resonates in the same region as lipids, and because the latter signals were very intense, weak signal intensity contribution from Lac might have been overshadowed by the broad lipid peaks. Second, we used a conventional spectroscopy pulse sequence in this study and therefore could not separate Lac signal intensity from that of lipids. Special Lac editing techniques may be required for the separation of Lac and lipids, and these methods have recently been proved successful in the evaluation of Lac for signs of hypoxia in head and neck tumors in vivo (16, 17).

As noted in the introduction, the technique of in vivo ^{1}H MR spectroscopy of head and neck tumors encounters many technical difficulties, especially at the skull base. The NPC lesions selected in this study were all >1 cm^3, and the success rate for interpretable spectra would have been lower had we included smaller lesions for study. Patient motion is another factor that may adversely affect spectral quality, and the non-interpretable spectra in this study were the result of patient motion (Table 1). Recently, motion correction procedures have been implemented in point-resolved spectroscopy-based localization sequences for ^{1}H MR spectroscopy of the body to correct for motion-induced phase variations (18). Finally, suboptimal shimming may be more difficult to overcome for primary tumors at the skull base, compared with nodes, because of low magnetic field inhomogeneity across the nasopharynx.

Despite these difficulties, in vivo ^{1}H MR spectroscopy has several advantages over in vitro ^{1}H MR spectroscopy studies. It is noninvasive, can be performed at the same time as conventional staging scanning, samples a greater volume of tissue, and has the potential to examine the true chemical composition of the tumor without the metabolites being influenced by changes in oxygenation when the tumor is removed. In addition, in vivo ^{1}H MR spectroscopy can sample areas that may not be accessible to biopsy, such as those around the skull base. Advances in in vivo spectroscopy, including the use of higher field magnets (3.0 T) to improve signal intensity-to-noise ratios and spectral resolution, together with parallel imaging (19) to overcome some of the effects of tissue susceptibility may provide hope for the clinical application of this technique in the future.

The primary treatment for NPC is radiation therapy, and after treatment, an indeterminate residual mass may be identified by CT or MR imaging. This is a particular problem with large primary tumors that have invaded outside the nasopharyngeal walls superiorly into the skull base or laterally into the parapharyngeal regions, areas that are usually inaccessible to biopsy. The problem is compounded in that the clinician prefers not to wait for tumor spread before confirming cancer in this vital region yet does not want to administer further radiation therapy considering the substantial radiation dose already delivered to adjacent vital organs, such as the temporal lobes, brain stem, and optic pathway. At present, fluorine-18-fluorodeoxyglucose positron emission tomography (20) shows promise in this area but is hindered by both false-positive and false-negative results. If further research reveals that the ^{1}H-spectra of residual NPC differs from that of post-radiation granulation tissue/fibrosis, spectroscopy offers the prospect of a

new valuable diagnostic tool. However, the difficult site of these indeterminate masses and their often small and irregular shapes means that in clinical practice, they are often not amenable to the current techniques for spectroscopic examination.

In conclusion, this is a preliminary study and further studies with a larger patient population may be needed to verify our results. However, we have shown that ^{1}H MR spectroscopy is a feasible technique with which to investigate NPC lesions >1 cm^3 and that interpretable spectra can be acquired at the skull base by using a standard receiver coil. The technique shows potential as a new diagnostic tool in the evaluation of NPC, with initial results showing that both primary cancer and metastatic nodes have higher Cho/Cr ratios compared with normal muscle tissues.

References

1. Smith IC, Stewart LC. **Magnetic resonance spectroscopy in medicine: clinical impact.** *Prog Nucl Magn Reson Spectroscopy* 2002;40: 1–34
2. Star-Lack JM, Adalsteinsson E, Adam MF, et al. **In vivo 1H MR spectroscopy of human head and neck lymph node metastasis and comparison with oxygen tension measurements.** *AJNR Am J Neuroradiol* 2000;21:183–193
3. Mukherji SK, Schiro S, Castillo M, Kwock L, Muller KE, Blackstock W. **Proton MR spectroscopy of squamous cell carcinoma of the extracranial head and neck: in vitro and in vivo studies.** *AJNR Am J Neuroradiol* 1997;18:1057–1072
4. Huang W, Roche P, Shindo M, Madoff D, Geronimo C, Button T. **Evaluation of head and neck tumor response to therapy using in vivo 1H MR spectroscopy: correlation with pathology.** *Proc Int Soc Magn Reson Med* 2000;8:552
5. Maheshwari SR, Mukherji SK, Neelon B, et al. **The choline/creatine ratio in five benign neoplasms: comparison with squamous cell carcinoma by use of in vitro MR spectroscopy.** *AJNR Am J Neuroradiol* 2000;21:1930–1935
6. Vanhamme L, van den Boogaart A, van Huffel S. **Improved method for accurate and efficient quantification of MRS data with use of prior knowledge.** *J Magn Reson* 1997;129:35–43
7. Van den Boogaart A, van Ormondt D, Pijnappel WWF, de Beer R, Ala-Korpela M. **Removal of the water resonance from H-1 magnetic resonance spectra.** In: McWhirter JG, ed. *Mathematics in Signal Processing III.* Oxford: Clarendon; 1994:175–195
8. Bezabeh T, El-Sayed S, Ahmed N, et al. **Correlating MR spectral features with histopathology in squamous cell carcinoma of the head and neck region.** *Proc Int Soc Magn Reson Med* 2000;8:551
9. Bezabeh T, Odlum O, Patel R, et al. **Predicting prognosis and clinical outcome in head and neck tumors: a spectroscopic approach.** *Proc Int Soc Magn Reson Med* 2002;10:2050
10. Miller BL. **A review of chemical issues in 1H NMR spectroscopy: *N*-acetyl-L-aspartate, creatine and choline.** *NMR Biomed* 1991;4: 47–52
11. van Zijl PC, Moonen CT, Gillen J, et al. **Proton magnetic resonance spectroscopy of small regions (1 mL) localized inside superficial human tumors: a clinical feasibility study.** *NMR Biomed* 1990;3: 227–232
12. Yeung DK, Cheung HS, Tse GM. **Human breast lesions: characterization with contrast-enhanced in vivo proton MR spectroscopy: initial results.** *Radiology* 2001;220:40–46
13. Bezabeh T, El-Sayed S, Odlum O, et al. **Grading of head and neck tumors by 1H MRS: an approach with potential clinical utility.** *Proc Int Soc Magn Reson Med* 2001;9:2345
14. Mukherji SK, Schiro S, Castillo M, et al. **Proton MR spectroscopy of squamous cell carcinoma of the upper aerodigestive tract: in vitro characteristics.** *AJNR Am J Neuroradiol* 1996;17:1485–1490
15. EI-Sayed S, Bezabeh T, Odlum O, et al**. An ex vivo study exploring the diagnostic potential of 1H magnetic resonance spectroscopy in squamous cell carcinoma of the head and neck region.** *Head Neck* 2002;24:766–772
16. Adalsteinsson E, Spielman DM, Pauly JM, Terris DJ, Sommer G, Macovski A. **Feasibility study of lactate imaging of head and neck tumors.** *NMR Biomed* 1998;11:360–369
17. Star-Lack J, Spielman D, Adalsteinsson E, Kurhanewicz J, Terris DJ, Vigneron DB. **In vivo lactate editing with simultaneous detection of choline, creatine, NAA, and lipid singlets at 1.5 T using PRESS excitation with applications to the study of brain and head and neck tumors.** *J Magn Reson* 1998;133:243–254
18. Star-Lack JM, Adalsteinsson E, Gold GE, Ikeda DM, Spielman DM. **Motion correction and lipid suppression for 1H magnetic resonance spectroscopy.** *Magn Reson Med* 2000;43:325–330
19. Dydak U, Weiger M, Pruessmann KP, Meier D, Boesiger P. **Sensitivity-encoded spectroscopic imaging.** *Magn Reson Med* 2001;46: 713–722
20. Kao CH, Shiau YC, Shen YY, Yen RF. **Detection of recurrent or persistent nasopharyngeal carcinomas after radiotherapy with technetium-99m methoxyisobutylisonitrile single photon emission computed tomography and computed tomography: comparison with 18-fluoro-2-deoxyglucose positron emission tomography.** *Cancer* 2002;94:1981–1986